Cell. Mol. Life Sci. 63 (2006) 1266–1277
1420-682X/06/111266-12
DOI 10.1007/s00018-005-5447-y

Cellular and Molecular Life Sciences

Review

Light-driven DNA repair by photolyases

L. O. Essen* and T. Klar

Department of Chemistry, Philipps University, Hans-Meerwein-Strasse, 35032 Marburg (Germany),
Fax: +49 6421 2822191, e-mail: essen@chemie.uni-marburg.de

Received 29 September 2005; received after revision 30 November 2005; accepted 15 February 2006
Online First 15 May 2006

Abstract. DNA photolyases are highly efficient light-driven DNA repair enzymes which revert the genome-damaging effects caused by ultraviolet (UV) radiation. These enzymes occur in almost all living organisms exposed to sunlight, the only exception being placental mammals like humans and mice. Their catalytic mechanism employs the light-driven injection of an electron onto the DNA lesion to trigger the cleavage of cyclobutane-pyrimidine dimers or 6-4 photoproducts inside duplex DNA. Spectroscopic and structural analysis has recently yielded a concise view of how photolyases recognize these DNA lesions involving two neighboring bases, catalyze the repair reaction within a nanosecond and still achieve quantum efficiencies of close to one. Apart from these mechanistic aspects, the potential of DNA photolyases for the generation of highly UV-resistant organisms, or for skin cancer prevention by ectopical application is increasingly recognized.

Keywords. DNA-photolyase, cyclobutane-pyrimidine dimer (CPD), base flipping, DNA repair, electron transfer, blue-light reactions, ultraviolet radiation, skin cancer.

Introduction

Ultraviolet radiation, especially UV-B (290 nm < λ < 320 nm), endangers all forms of sun-exposed life by the formation of various genotoxic photoproducts in DNA which subsequently cause mutations, growth delay or even killing [1, 2]. To ensure genetic integrity when living cells are exposed to bright sunlight, nature invented several strategies to repair different types of UV damage. The two major UV-induced lesions (Fig. 1a) are cis-syn cyclobutane pyrimidine dimers (CPDs) and pyrimidine-pyrimidone (6-4) photoproducts (6-4 PPs). These lesions mostly exert their detrimental cytotoxic effects by blocking DNA replication and transcription and are the major players in the formation of skin cancers [3]. *In vivo* the CPD and 6-4 PP lesions are formed in a ratio of about 3:1 [4] from two, in a DNA strand adjacently located pyrimidine bases, mainly thymine. Their enzymatic repair (Fig. 1a) involves the catalytic cleavage of the pyrimidine dimers using near-UV or blue light (λ = 320–500 nm) and was first reported more than 50 years ago as photoreactivation [5, 6]. The enzyme that enables the light-driven repair of UV-damaged DNA was afterwards found to be a flavoprotein and the term 'photoreactivating enzyme' changed to DNA photolyase [7, 8]. DNA photolyases represent one of only two known classes of light-driven enzymes in nature, the other being the light-driven and NAD(P)H-dependent protochlorophyllide oxidoreductases [9] which catalyze the final step in chlorophyll biosynthesis in photosynthetic organisms. Due to their ability to repair two different lesion types, DNA photolyases are classified either as CPD photolyases or as (6-4) photolyases.

The following review will mostly focus on aspects not covered to any extent in two previous and excellent reviews on DNA photolyases [10, 11].

* Corresponding author.

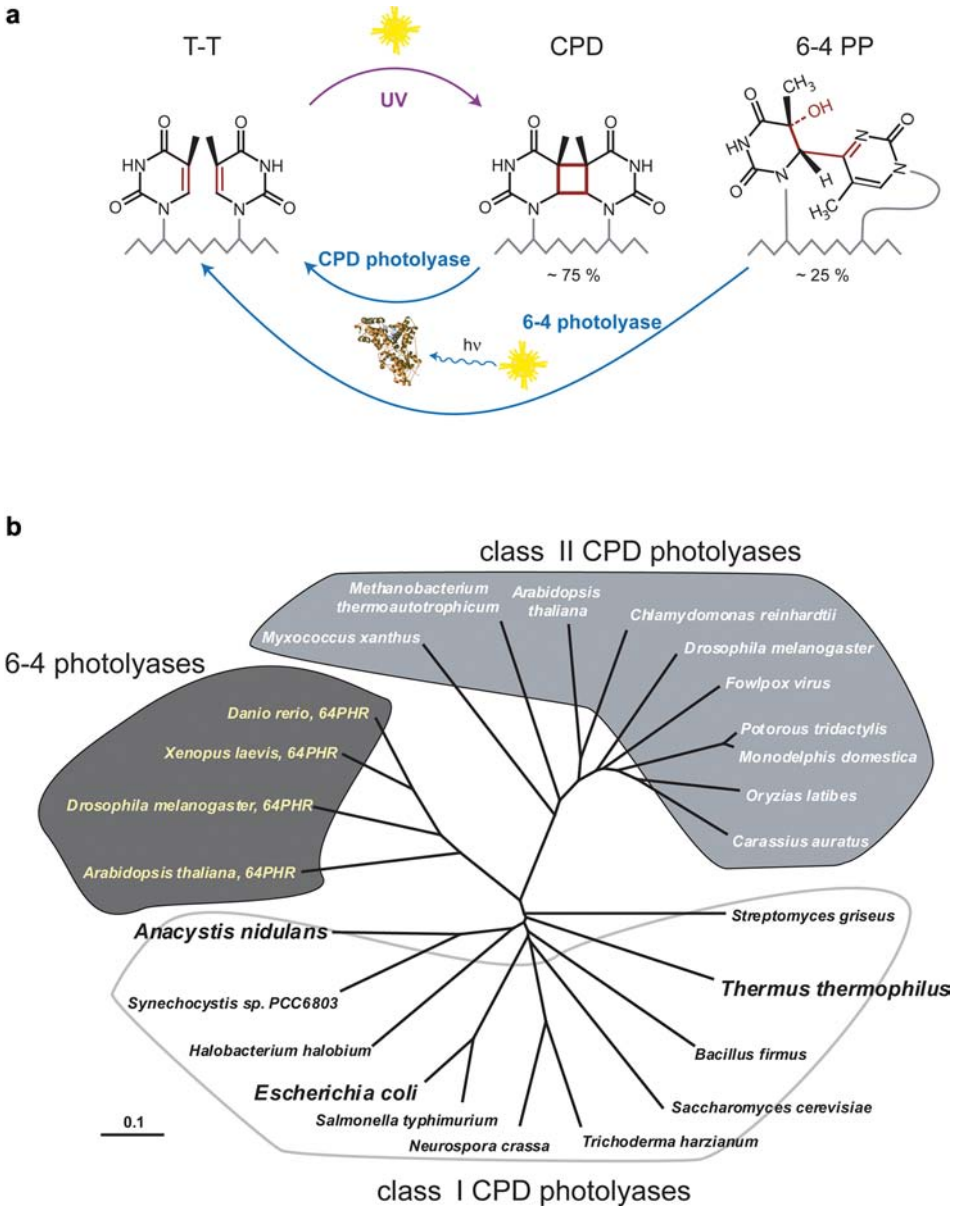

Figure 1. (*a*) Formation and enzymatic repair of the primary UV lesions, the cyclobutane pyrimidine dimers (CPD) and the 6-4 pyrimidone-pyrimidine adducts (6-4 PP). (*b*) Dendrogram showing the sequence relationships within the photolyase subfamilies. So far, only crystal structures from class I photolyases (highlighted in bold) have been solved.

Evolution and structural organization of DNA photolyases

During the Archaean era (2.5–3.8 Ga ago) the lack of a UV-protective ozone layer around Earth caused the passage of unfiltered solar UV-C radiation (λ ~ 190–280 nm) down to the surface and the upper layers of the global oceans [12]. The DNA-damaging UV flux at that time was estimated to be about three orders of magnitude larger than the flux today, and thus limited the survival and growth of organisms in the photic region of the oceans. Given these circumstances, it is not surprising that DNA photolyases emerged in all three kingdoms of life: archaea, eubacteria and eukaryotes. The ancestral photolyase was probably present in the common progenitor of life and diversified by at least eight gene duplications to the families of photolyases and non-catalytic cryptochromes known today [13]. However, during a period of prebiotic evolution, the maintainance of sequence information in a pool of RNA species may not have depended at all on the catalytic function of protein-based DNA photolyases, because RNA, compared to DNA, is highly resistant against UV-induced lesions [14] and the sequence context might contribute to UV resistance or even to self-repair. The latter was demonstrated by a

study where *in vitro* selection of DNA sequences capable of light repair succeeded to yield a 42-nucleotide-long DNA fragment that underwent self-repair if illuminated by near-UV light [15].

DNA photolyases are monomeric proteins 45–66 kDa in size, and comprise 420–616 amino acid residues. Dependent on the substrate specifity, photolyases can be classified into two groups. CPD photolyases or DNA photolyases repair CPD lesions in single- and double-stranded DNA. (6-4) pyrimidine-pyrimidone dimers are cleaved by (6-4) photolyases. The CPD photolyases are further subdivided into two classes whose members share sequence identities of less than 20% if derived from different classes, but more than 30–35% if selected from the same class (Fig. 1b). Class I DNA photolyases are widely found in eubacteria, fungi and haloarchaea [16]. In contrast, class II DNA photolyases occur in eukaryotes other than fungi as well as in a few eubacteria [17], several pathogens like poxviruses [18, 19] and some parasitic microsporidiae [20]. In sponges, a CPD-like photolyase has been described that shared sequence similarity with the cryptochrome/6-4 photolyase family, but exhibited the activity of a typical CPD photolyase [21]. Overall, the spread of photolyase genes into the different branches of life was apparently at least partly driven by horizontal gene transfer.

DNA binding is apparently not only a feature of the catalytic DNA photolyases, but also occurs in the structurally highly related cryptochromes, although the physiological function of DNA binding is still unresolved in these blue-light-triggered signaling proteins. For example, the DASH cryptochromes which form a separate subfamily among the photolyases/cryptochromes [22, 23] bind DNA with rather low affinity. The human cryptochrome Cry2 [24] likewise binds non-specifically to DNA but, interestingly, with a higher affinity to 6-4-PP-lesion-containing DNA without effecting its light-driven repair. Furthermore, human Cry2 binds preferentially to ssDNA ($K_D \sim 5$ nM) than to dsDNA, whereas CPD DNA photolyases do not exhibit such a preference. Given the very close sequence relationship between 6-4 photolyases and animal cryptochromes (pairwise sequence identities: ~40–60%), this DNA-binding activity has been speculated to be the base for some of the transcriptional control activity of animal cryptochromes.

Until now, only the crystal structures of the class I photolyases from *Escherichia coli* [25], the cyanobacterium *Anacystis nidulans* [26] and *Thermus thermophilus* [27] have been solved at resolutions between 1.8 and 2.3 Å (Table 1). Like the structurally related cryptochromes from *Synechococcus* sp. and *Arabidopsis thaliana* [23, 28], these structures reveal a common architecture, with

Table 1. X-ray crystallographic characterization of DNA photolyase and cryptochrome structures.

PDB code	Protein	Organism	Resolution Å	Reference	Remark
1DNP	DNA photolyase	*Escherichia coli*	2.30	25	complexed with MTHF antenna pigment
1IQR	DNA photolyase	*Thermus thermophilus*	2.10	27	no antenna pigment observed
1IQU	DNA photolyase	*Thermus thermophilus*	2.20	27	complexed to thymine base in active site
1QNF	DNA photolyase	*Anacystis nidulans*	1.80	26	complexed with 8-HDF antenna pigment
1OWL	DNA photolyase	*Anacystis nidulans*	1.80	37	apoenzyme, i.e. without 8-HDH antenna pigment
1OWM	DNA photolyase	*Anacystis nidulans*	2.30	37	apoenzyme; received X-ray dose of 1.2×10^{15} photons/mm^2
1OWN	DNA photolyase	*Anacystis nidulans*	2.30	37	apoenzyme; received X-ray dose of 4.8×10^{15} photons/mm^2
1OWO	DNA photolyase	*Anacystis nidulans*	2.30	37	photoreduced apoenzyme; received X-ray dose of 1.2×10^{15} photons/mm^2
1OWP	DNA photolyase	*Anacystis nidulans*	2.30	37	photoreduced apoenzyme; received X-ray dose of 4.8×10^{15} photons/mm^2
1TEZ	DNA photolyase	*Anacystis nidulans*	1.80	38	complex with bound CPD-containing dsDNA and 8-HDF
1NP7	cryptochrome DASH	*Synechocystis* sp. PCC6803	1.90	23	no antenna pigment observed
1U3C	Phr domain of Cry1	*Arabidopsis thaliana*	2.60	28	no antenna pigment observed
1U3D	Phr domain of Cry1	*Arabidopsis thaliana*	2.45	28	complexed to non-hydrolyzable ATP analog AM PP(NH)P

a larger C-terminal, all α-helical domain (240–280 residues) that harbors the catalytic cofactor FAD and an N-terminal α/β domain (180–220 residues). The latter comprises a Rossman fold with a five-stranded, parallel β sheet and is mostly responsible for the versatile binding of additional antenna pigments (Fig. 2a). Despite the early emergence of photolyases during evolution there are no close structural homologs for the C-terminal catalytic domain outside the photolyase/cryptochrome families where this fold found other use.

The catalytic FADH$^-$ cofactor of photolyases

All photolyases and cryptochromes comprise FAD as a light-sensitized cofactor and chromophor. In photolyases, this cofactor transfers after excitation an electron transiently to the DNA lesion to trigger its repair by a radical mechanism. The catalytic FAD cofactor is unusually bound in the C-terminal domain by adopting a U-shaped conformation that allows the adenine moiety to contact the redox-active isoalloxazine group (Fig. 2a, b). This conformation had not been previously observed in any other flavoprotein and apparently reflects the unique mode of catalysis (see below). To achieve its active state, this flavin is reduced by a light-driven process to a deprotonated FADH$^-$ species [29]. In its reduced and oxidized states, the deprotonated N3 nitrogen of the isoalloxazine forms an intramolecular hydrogen bond with the 3′-hydroxyl group of the ribityl chain. The FAD-binding site is highly conserved among the photolyase and cryptochrome structures. In the class I structures and the reported cryptochrome structures of Cry1 from *A. thaliana* [28] and of cry-DASH from *Synechococcus* sp. [23], the isoalloxazine ring is sandwiched between a salt bridge comprising an arginine and an aspartate residue (e.g. *A. nidulans:* R352/D380; *E. coli:* R344/D372) and short polypeptide stretches (*A. nidulans*/*E. coli:* A385-N386/A377-N378, G389-W390/G381-W382). Another conserved interaction is a hydrogen bond formed between the N5 nitrogen of the isoalloxazine group and a conserved asparagine sidechain (*A. nidulans*/*E. coli:* N386/N378).

Interestingly, the reduction of the catalytic cofactor is, like the DNA repair, a process where the absorption of visible light by FADH$^\bullet$ or oxidized FAD triggers an electron transfer process from an exogenous electron donor onto the flavin [29]. Photoreduction of the flavin cofactor in the absence of added artificial photosensitizers is not entirely uncommon among flavoproteins. For example, homologs of the old yellow enzyme also undergo photoreduction to a fully reduced flavin species via the semichinoid form [30]. However, due to the simplicity of the experimental system, the electron transfer pathway for this process in DNA photolyases has been biophysically studied in much detail during the last two decades [for a concise review see ref. 10]. Mutagenesis and ultrafast kinetic spectroscopy revealed a consecutive chain of three conserved tryptophan residues with the order W306 $\rightarrow$ W359 $\rightarrow$ W382 $\rightarrow$ FAD(H$^\bullet$) in the *E. coli* enzyme, and Y469 (?) $\rightarrow$ W314 $\rightarrow$ W367 $\rightarrow$ W390 $\rightarrow$ FAD(H$^\bullet$) in the *A. nidulans* photolyase. In the *E. coli* enzyme, reduction of FADH$^\bullet$ and subsequent appearance of a deprotonated Trp$^\bullet$ radical is accomplished within 5 µs [31]. As the reverse electron transfer leading to charge recombination is significantly slower (~17 ms) and apparently inhibited by deprotonation of the terminal surface-exposed tryptophan residue (*E. coli* W306), there remains sufficient time to subtract an electron from an exogenous electron source. Variations on this theme were found for the *A. nidulans* photolyase [32], the 6-4 photolyase from *A. thaliana* [33] and Cry1 from *A. thaliana* [34] where tyrosine radical species were additionally delineated during photoreduction of the flavin cofactor. There is also some evidence for redundant electron transfer pathways. Kinetic studies on the *E. coli* photolyase indicated that the photoreduction of the catalytic flavin can also proceed via electron-hopping along helix α-15 and an aromatic residue (F366) contacting the flavin [35].

The three-tryptophan electron transfer pathway for photoreduction of the FAD cofactor is structurally not only conserved in 6-4 and most likely also in class II photolyases, but could be delineated as well in the cryptochrome structures [23, 28]. A photocycle-like behavior was first described for the Cry1 cryptochrome from *A. thaliana* [34]. Here, a signaling role for the photoreduction process was demonstrated by tryptophan mutants of Cry1, which showed a loss of light-driven signaling *in vitro* and *in vivo* [36]. Accordingly, the light-driven change of the redox state of the FAD cofactor from a fully oxidized to a reduced state is now thought to promote the formation of signaling states in cryptochromes. However, structural changes at the flavin-binding site alone are unlikely to be sufficient to trigger a signaling state which might interact with downstream components of the cryptochrome signaling pathways. X-ray crystallographic data from the *A. nidulans* photolyase [37, 38] showed only minor conformational changes upon reduction of the catalytic flavin, mainly an increased butterfly-like bending of the isoalloxazine moiety. Currently, one can only speculate that long-range electron transfer events from aromatic residues and/or pK changes at the protein surface are responsible for the local structural changes required for modulating cryptochrome-protein interactions.

The light-antenna of DNA photolyases

At the interface between the catalytic C-terminal and the N-terminal α/β domain, methenyltetrahydrofolate (MTHF) or an 8-hydroxydeazaflavin (8-HDF) were observed as ancillary chromophores in the structures of the *E. coli* [25] and *A. nidulans* enzyme, respectively

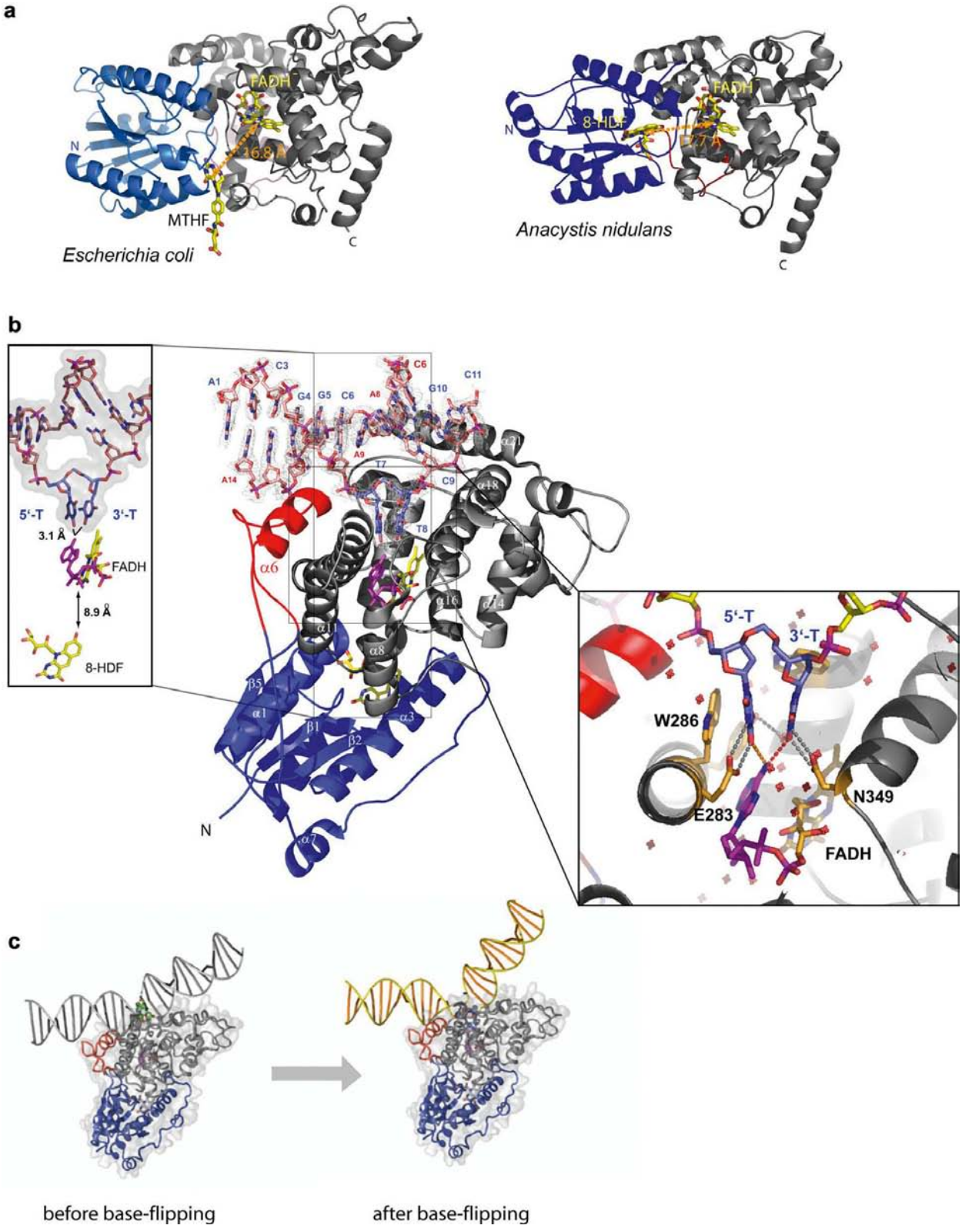

Figure 2. (*a*) The antenna-pigment-binding site for photolyases of the MTHF type (left, *E. coli*) and of the 8-HDF type (right, *A. nidulans*). (*b*) Complex between a CPD-containing duplex DNA and the class I photolyase from *A. nidulans*. (*c*) Structural models for the increase in the CPD-induced DNA bend induced by binding to DNA photolyase and base-flipping of the thymine dimer.

(Fig. 2a). In class I or II CPDs as well as in 6-4 photolyases, no other chromophore than MTHF and 8-HDF has yet been described. For many of the characterized and mostly recombinant DNA photolyases, the nature of their antenna pigments is still not known. This apparent lack of an antenna pigment chromophore in several CPD photolyases, e.g. the class II CPD photolyase from *A. thaliana* [39], does not imply that these photolyases lack an antenna chromophore *in vivo*. Action spectra for the CPD lesion repair in sorghum, cucumber [40] and maize [41] indicated a maximum at 400 nm which might be consistent with an MTHF chromophore (λ_{max} ~ 380 nm) that experiences a protein-induced red shift, as observed in the *Bacillus firmus* enzyme [42].

Due to the low extinction coefficients of the reduced $FADH^-$ chromophore in the visible region, these chromophores considerably broaden the action spectra and optical cross-sections of the DNA photolyases. The protein-chromophore interaction fine-tunes the optimal absorption characteristics, because the antenna pigments bind to the interfacial regions between the N-terminal and the catalytic domains with a concomitant bathochromic shift of their absorption. For example, in the *E. coli* photolyase, the MTHF absorbtion spectrum is red-shifted by 25 nm from 358 nm to 383 nm [43] by the interaction with an acidic residue of the antenna pigment binding site (*E. coli* E109). Due to the proximity of the antenna pigments, 16.8 Å between MTHF and $FADH^-$ in the *E. coli* enzyme and 17.7 Å between 8-HDF and $FADH^-$ in the *A. nidulans* photolyase, the transfer of excitation energy is very rapid and apparently follows a Förster-type mechanism. In the *E. coli* enzyme transfer rates of 292 ps and 19 ps were determined for the excitation transfer from MTHF to the reduced and semichinoid catalytic flavin, respectively [35]. Similar short rates, 50 ps and < 20 ps, were reported for the excitation transfer from the 8-HDF antenna pigment of the *A. nidulans* photolyase to $FADH^-$ and $FADH^\bullet$, respectively [44]. The measured rates are quite compatible with the measured distances and relative orientations between the antenna pigments and the catalytic flavin.

Together with the high quantum yields of 0.62 and 0.94 for excitation transfer in the class I photolyases [44], one may conclude that the photolyases are not only the simplest light-harvesting systems in nature, but can favorably compete with the highly complex photosynthetic units. Whether the chemical nature of the antenna pigments in photolyases can be now chemically manipulated for changing even further the absorption and DNA repair characteristics of these enzymes remains to be seen.

DNA recognition by DNA photolyases

If not sterically hindered by the packing of DNA around nucleosomes [45], DNA photolyases recognize CPD lesions with rather high affinity in single- or double-stranded DNA, e.g. the *E. coli* photolyase exhibits dissociation constants of ~10^{-8} M for both forms of DNA. Although there is no sequence dependence for the repair of CPD lesions, the binding of the thymine dimer only contributes half of the binding energy (K_D ~ 10^{-4} M), the other half being contributed by the deoxyphosphate-ribose backbone of the DNA strand. Structural information about the interaction between CPD lesions and photolyases became available recently from X-ray crystallography [38] and nuclear magnetic resonance (NMR) spectroscopy [46, 47]. The 1.8-Å X-ray structure of a complex between the *A. nidulans* photolyase and a CPD lesion comprising duplex DNA corroborated earlier data from atomic force microscopy [48] by showing that the enzyme increases the CPD-induced kink in the B-type DNA upon binding from about 20–30° [49, 50] to 50°. The large kinking of the B-type DNA is accompanied by a flip-out of the CPD lesion into the active site of the enzyme such that the thymine dimer is suitably positioned to form hydrogen bonds between the C4 carbonyls and the N6 amino group from the adenine moiety of the catalytic $FADH^-$ (Fig. 2b). This intimate mode of interaction was not predicted by several modeling studies [51–53] and, interestingly, also not by an NMR spectroscopic characterization of CPD-DNA binding to the *T. thermophilus* photolyase [46]. Here, paramagnetic resonance enhancement (PRE) from the catalytic FAD in its semiquinone form was used as a novel technique to trigger NMR resonance changes in the CPD lesion. The estimated distance parameters between FAD and the CPD lesion amounted to 16 ± 3 Å. Although a flipping-out of the CPD lesion could be likewise delineated by the NMR techniques [46, 47], only a peripheral docking of the CPD lesion was predicted along the entrance of the active site. Further indications for a close interaction between the CPD lesion and the adenine group of the $FADH^-$ cofactor were found by the increase of the mid-point potential of the redox pair $FADH^-/FADH^\bullet$ from 16 to 81 mV upon substrate binding [54] and a concomitant 1.8-fold speed-up for intraprotein electron transfer from $FADH^-$ to the surface-exposed tryptophan radical $W306^\bullet$ in the *E. coli* enzyme [55].

Salt bridges and hydrogen bonds are extensively formed along the protein surface and the phosphates P^{-1}, P^{+1}, P^{+2} and P^{+3} [38, 47]. Although the synthetic CPD lesion of the photolyase/CPD-DNA cocrystal structure comprises a formacetal group instead of the intradimer phosphate P^0, major interactions with the missing P^0 phosphate are unlikely to occur because no residues are found in close proximity which are capable of forming H bonds or salt bridges. This lack of interaction with P^0 is consistent with protection assays which defined a NpT <> TpNpNp signature as a common signature motif of DNA binding by photolyases [56, 57]. The crucial role of these interactions (Fig. 3) for the formation of a catalytically compe-

tent photolyase/CPD-DNA complex is underlined by a mutation of a conserved arginine (*A. nidulans*/*E. coli:* R350/R342), which forms a salt bridge with P^{+1} [58]. Among several active-site mutants this R→A mutant was found to exhibit the greatest effect by lowering the selectivity toward CPD-containing DNA 32-fold and the quantum yield of CPD cleavage from 98% to about 60%. In contrast, mutations of residues interacting with P^{+2} (*A. nidulans/E. coli:* Q411/Q403, K414/K406) only affected the affinity toward CPD-containing DNA [58]. Furthermore, the helical segment α6 protrudes into the minor groove at the 5′ end of the CPD lesion. As in several other DNA-binding proteins, DNA photolyases seem to utilize the dipolar moment of this helix for electrostatic stabilization of the protein-DNA complex by directing the N terminus of α6 toward the P^{-1} phosphate. A similar helix dipole-ion interaction may be postulated for helix α18 that points toward the P^{+2} phosphate.

The α6 helix belongs to a long protrusion that emerges from the N-terminal domain (Figs. 2b, 3). Unlike the remainder of the N-terminal domain, this region does not contribute to the binding of the antenna pigment, but interacts with the non-CPD-containing strand by hydrogen bonding with the P^{-4} and P^{-5} phosphates of the backbone. These interaction sites on the non-CPD strand are supplemented by a Mg^{2+}-bridged interaction between P^{-3} and a conserved aspartate (*A. nidulans/E. coli:* D399/D391). According to DNA protection assays [57], the interaction sites on the non-CPD strand are conserved among the sequence-divergent class I and II photolyases. Interestingly, the DNA-binding protrusion motif is structurally conserved in cryptochromes of the DASH subfamily, which also bind to duplex DNA, but lack any repair capability [23]. Another, but generally not conserved salt bridge with the non-CPD strand is formed between K472 and the P^{-1} phosphate. As the affinity of DNA photolyases is not higher for double-stranded DNA than for single-stranded DNA [11], the interactions with the non-CPD strand might compensate the additional energetic costs of extensive DNA bending and base-flipping during formation of the enzyme-substrate complex.

Despite the structural information about the DNA/photolyase complex and the high affinities of CPD DNA photolyases, how DNA photolyases find the lesions in duplex DNA is still not clear. Crystal and NMR structures of duplex DNA with CPD lesions [50, 59] show only minor distortions of B-type DNA with the thymine dimer still being base-stacking and forming three out of four hydrogen bonds with the complementary adenine bases. Molecular dynamics simulations showed that the presence of a CPD lesion at least increases the flexibility of the B-type DNA around the lesion site [60], making it more prone to base-

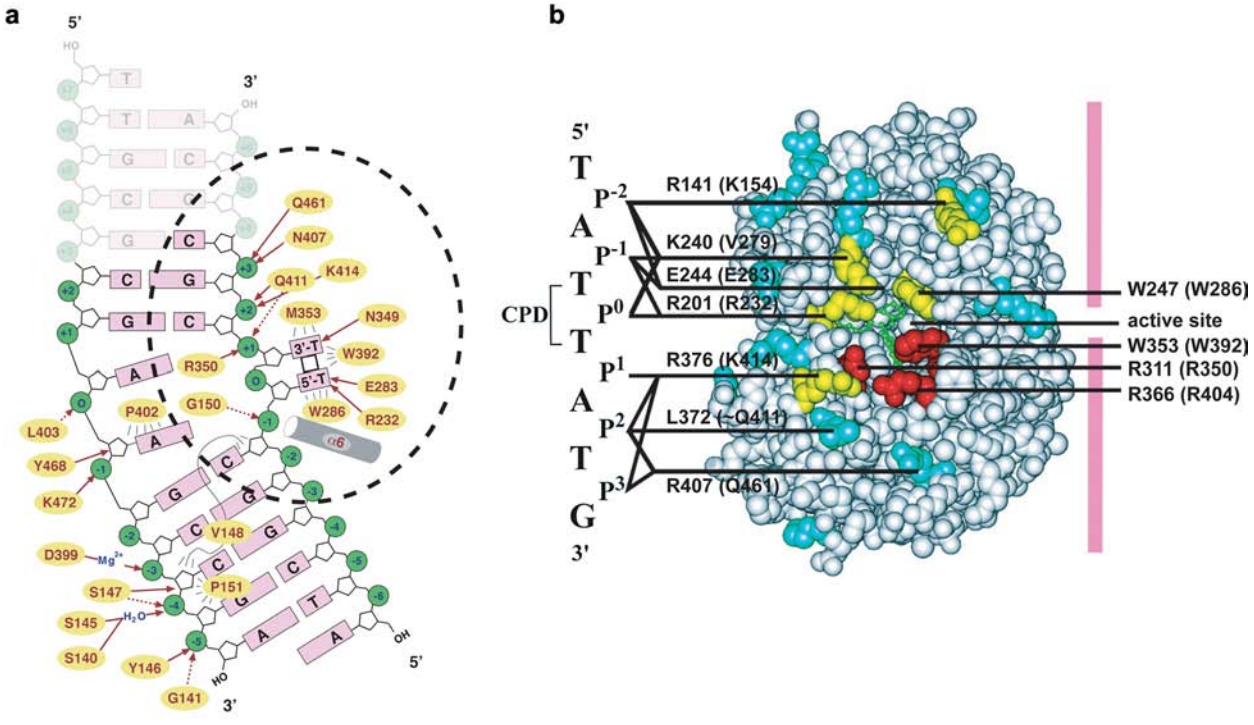

Figure 3. Schematic representation of interactions between CPD-lesion-containing DNA and class I photolyases as revealed for the *A. nidulans* enzyme by X-ray crystallography [38] (*a*) and for the *T. thermophilus* photolyase by NMR spectroscopy [47]. (*b*) For a better comparison of the common binding mode of the duplex DNA in the *A. nidulans* photolyase and of the single-stranded oligonucleotide in the *Thermus* enzyme, the numbers in parentheses correspond to the *A. nidulans* numbering. *b* modified from Torizawa et al. [47] with permission.

flipping or structural deformation. Recognition motifs in CPD-lesion-containing DNA might be the higher-energy BII conformation of the backbone at the 3′ side of the CPD lesion [50, 59] and a change in the intraphosphate distances which might favor the recognition of the P^{-1}, P^{+1}, P^{+2} and P^{+3} phosphates by the enzyme.

Another contribution might arise from a flexible, non-regular ridge (*A. nidulans:* G397-F406) which penetrates between the DNA strands upon double-flipping of the thymine dimer into the active site. This disruption creates a hole of about 10×10 Å that is mostly filled by this ridge making non-specific van der Waals interactions with the adenines complementary to the CPD lesion. Other specific interactions are missing, apart from a hydrogen bond between the P^0 phosphate of the complementary strand and a main-chain peptide group. At least in class I photolyases, this ridge might be a passive and flexible space filler, because it exhibits increased thermal mobility in all other structures of non-complexed DNA photolyases [25–27]. Due to the lack of specific interactions, the adenine ring complementary to the 5′ T of the CPD lesion is highly accessible to methylation in *E. coli* photolyase [57]. However, sequence variation in the ridge region may affect DNA binding, because in the class II enzyme from *Methanobacterium thermoautotrophicum* the affinity is not only increased by two to three orders of magnitude ($K_D \sim 10^{-11}$ M), mostly by decreasing the dissociation rate k_{off}, but the complementary adenine becomes also efficiently protected against methylation [57].

Mechanism of DNA photolyases

After DNA binding and double-flipping of the CPD lesion into the active site, the repair of DNA occurs by light-driven injection of an electron from the excited $FADH^{-}$* to the CPD lesion (Fig. 4a). About 125 kJ/mol of the 240 kJ/mol of energy that is captured upon photon absorption is consumed during this initial electron transfer step [61]. After electron capture, the splitting of the CPD lesion proceeds rapidly within 0.6 ns [62, 63]. This is about 10^3-fold faster than the non-catalyzed rate of splitting an anionic CPD radical and indicates that the active site distorts the CPD lesion in a manner that splitting of the CPD is promoted, e.g. by increasing the strain in the cyclobutane ring. The rapid electron transfer rate, now precisely determined to 0.17 ns [62], might be aided by the electric dipole moment of the CPD substrate as the CPD thymines make hydrogen bonds with the catalytic $FADH^{-}$ cofactor [38]. This intimate interaction between the CPD lesion and the catalytic flavin was found in several instances to affect the kinetics of electron transfer reactions [55, 64]. Interestingly, the X-ray structure of the photolyase/CPD-DNA complex showed the synthetic CPD lesion in its repaired state as the synchrotron radiation used during crystallographic data collection repaired the CPD lesion in the crystals, presumably by the radiation-mediated release of free electrons [38]. The repaired CPD inside the active site was almost superimposable on a model of the intact CPD lesion, indicating that the radical anion cycloreversion, i.e. the splitting of the CPD lesion, proceeds without major reorientations of the CPD lesion during the whole reaction course.

The high quantum yields of many DNA photolyases of up to 0.98 [44] imply that non-productive back-transfer of the electron from the CPD lesion to the $FADH^{\cdot}$ radical that would otherwise cause a futile cycle is efficiently avoided by the enzyme before cleavage of the cyclobutane ring is completed. Nevertheless, back-transfer of the electron from the split thymine dimer onto the catalytic flavin cofactor has to be at the same time highly efficient in order to restore the activity of the enzyme. One possibility for achieving this would be to use separate electron transfer pathways where the reduction of the $FADH^{\bullet}$ cofactor occurs by separate photoreduction as discussed above. Ultra-fast femtosecond laser spectroscopy initially suggested that the photolyase was indeed left in the semiquinonid state after repair of the CPD lesion had been accomplished [63]. However, using a mutant of the *E. coli* photolyase (W306F) that is impaired in the photoreduction of the $FADH^{-}$, Sancar and colleagues could unambigously demonstrate that the intraprotein electron transfer pathway of the photoreduction process is not a regular part of the photolyase photocycle under physiological conditions, because the enzyme was able to undergo at least 25 repair cycles before losing activity [65]. Furthermore, a direct back-transfer of the excess electron from the thymine dimer to the $FADH^{\bullet}$ cofactor could be followed by ultra-fast spectroscopy with a time constant of 0.56 ns for CPD splitting and complete electron back-transfer [62].

From the structure of the photolyase/CPD-DNA complex, two routes for electron transfer from the catalytic flavin to the CPD lesion were apparent inside the active site [38] and consistent with the kinetic data. An indirect route along the hydrogen-bonded C4-carbonyls of the CPD lesion and the amino group of the adenine, or a direct route from the isoalloxazine to the CPD lesion, as both groups contact partially with a minimal distance of 4.3 Å. The former route can only play a role if a superexchange or tunneling mechanism is postulated for electron transfer, because the redox potential of adenines is lower than that of the CPD lesion (E_0 = –2.5 V vs. –1.4/–1.9 V). As the complex structure showed the CPD just after cleavage in the active site, the putative electron transfer routes are very likely maintained during the entire cleavage reaction. Solvation reordering with positional changes of water molecules and/or protein side chains was spectroscopically observed during the light-driven repair reaction [62]. One candidate for such an interac-

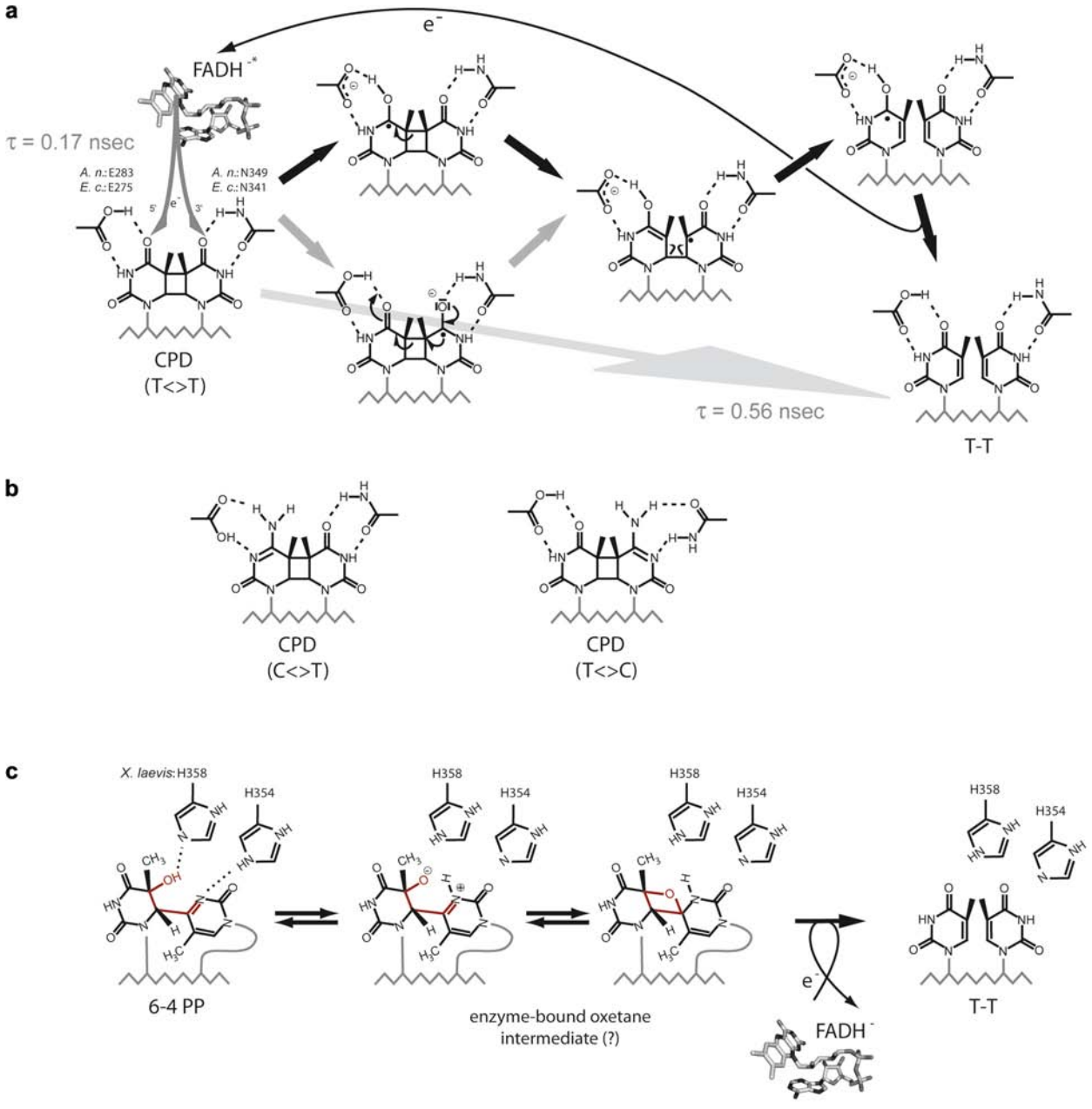

Figure 4. (*a*) Hypothetical repair mechanism of CPD photolyases involving transiently the protonation of the CPD radical anion. Note that this reaction sequence assumes a thymine dimer as CPD lesion. However, the repair of other CPD lesions like C <> T or T <> C is catalyzed by DNA photolyases as well. (*b*) Due to the almost symmetric recognition of the pyrimidines in the active site by a protonated glutamate and an asparagine residue, the binding of these lesions only requires a flip of the carboxylate or carboxamide groups to accomodate the alternative H-bonding pattern of cytosine bases. (*c*) Current hypothesis for the mechanism of 6-4 photolyases as suggested by Todo and coworkers for the *Xenopus laevis* 6-4 photolyase [71] that was based on an earlier model for general-acid/general-base-catalyzed formation of an enzyme-bound oxetane intermediate [70, 76].

tion between the substrate and the active that is affected during electron transfer might be the observed hydrogen bond between a protonated glutamic acid (*A. nidulans:* E283) and the O4 oxygen of the 5′ T base. A protonation of the electron-rich O4 group of the 5′ T upon protonation that is concurrent with electron transfer might be crucial to stabilize the radical anion CPD so that non-productive back-transfer of the electron onto the $FADH^{\bullet}$ radical is avoided and bond cleavage is favored (Fig. 4a). Quantum-chemical calculations [66] predicted that a protonated CPD radical should experience a significant thermal barrier for cleavage compared with the barrier-free dissolution of non-protonated CPD radical anions, but this thermal barrier might not exist in the context of the active site of the protein.

DNA photolyases also catalyze the cleavage of pyrimidine dimers comprising cytosines, albeit with an up to 20-fold reduced affinity and a twentyfold reduced quantum yield for the repair of C <> C lesions [67]. The quite promiscuous recognition of different pyrimidine dimers (T <> T ~ U <> U >> C <> C) in the active site may be facilitated by the almost symmetric interactions made by the carboxylate mentioned before with the 5′ T (*A. nidulans:* E283) and an asparagine (*A. nidulans:* N349) that likewise forms H bonds with the 3′ T. Cytosine bases in pyrimidine dimers would, hence, be expected to make similar interactions by flipping either the asparagine carboxamide group or forming an alternative H bond as shown in Figure 4b.

After DNA repair, the thymine pair has to flip back into the duplex DNA to form hydrogen bonds with the complementary adenines. This relaxation of the DNA backbone proceeds much more slowly than the repair of CPD lesions, as was shown by FTIR spectroscopy [68].

As the class I and II CPD DNA photolyases, (6-4) photolyases and cryptochromes are derived from a common ancestor, most likely of the CPD-type [13, 69], the pathway of electron injection into the DNA lesion should be a common feature among the members of this protein family. This pathway involving a hydrogen bond between the adenine amino group of the $FADH^-$ cofactor and the C4-carbonyl group of a pyrimidine sets tight restraints for the recognition mode of the 6-4 PP lesion by (6-4) photolyases. The 5′ T of this photoproduct is predicted to make similar interactions as the CPD damage, whereas the 3′ T may be hydrogen-bonded to a histidine (analogous to *A. nidulans* N349). Accordingly, binding of the 6-4 PP lesion to the enzyme is postulated to cause preferential formation of the oxetane-like species (Fig. 4b) that is otherwise unstable at temperatures above –80 °C [70]. Another histidine that corresponds to M353 in the *A. nidulans* photolyase was recently shown to affect catalysis [71] and supposed to act as a general acid with the 5′ T (Fig. 4c). However, due to the close spatial relationship in the active site, one might currently not exclude that this residue recognizes the P^{+1} phosphate by formation of a salt bridge, because in 6-4 photolyases the conserved arginine residue that forms the salt bridge to the P^{+1} phosphate in CPD-like photolyases (*A. nidulans* R350) is replaced by a leucine. These small differences around the active site presumably reflect the need for fine-tuning the DNA conformation on the protein surface to position the structurally divergent UV lesions precisely into the active sites of photolyases.

Perspectives on DNA photolyases for human health

Unlike other animals, the placental mammals lost light-driven DNA repair by CPD and 6-4 photolyases during evolution, presumably because the mammals were mostly small nocturnal animals until the end of the Cretaceous era when the dinosaurs were finally eradicated. In placental animals, the repair of CPD and 6-4 PP lesions is taken over by the nucleotide excision repair (NER) systems. Removal of 6-4 PP lesions in the genome occurs by global genome NER, whereas CPD lesions are only efficiently removed from transcription-active regions of the genome by transcription-coupled NER, and here preferentially from the transcribed strand. Human genetic diseases like xeroderma pigmentosum, trichothiodystrophy and Cockayne syndrome are therefore mostly related to defects in these NER systems. Recently, the beneficial effect of transfering a CPD photolyase into mammals was demonstrated, when transgenic mice were generated with a transgene for a marsupial CPD photolyase [72]. These mice exhibited a 40% increase of repair for CPD lesions in intact skin and cultured fibroblasts that was accompanied by an improved resistance against acute UV-induced effects like erythema (sunburn), epidermal hyperplasia or apoptosis. Most remarkably, the expression of the CPD photolyase in mice efficiently suppressed the formation of skin carcinomas. In contrast, the expression of a plant 6-4 PP photolyase [73] did not improve the resistance against carcinoma formation or lower the UV-B-induced mutation rate. Apparently, the endogenous global genome NER systems have a sufficient capacity to repair 6-4 PP lesions whereas the transcription-coupled NER is less effective against CPD lesions.

Surprisingly, the topical application of liposome formulations with CPD photolyases as an active biological ingredient onto human skin was reported to provide some protection against UV-B-induced damage like erythema and immunogenic hypersensitivity reactions [74]. However, in the absence of a functional NER, the carcinogenic potential of 6-4 PP lesions in humans is apparently severalfold larger than that of CPD lesions [75]. Therefore, whether additional protection against UV-induced CPD lesions is sufficient in humans to lower the rate of carcinoma formation awaits further investigations.

Acknowledgements. This work was supported by grants from the Deutsche Forschungsgemeinschaft (ES152/2) and the Volkswagen-Stiftung. The authors thank A. Batschauer for discussion and the provision of an earlier version of Figure 1b.

1 Vink A. A. and Roza L. (2001) Biological consequences of cyclobutane pyrimidine dimers. J. Photochem. Photobiol. B **65:** 101–104
2 Slaper H., Velders G. J., Daniel J. S., Gruijl F. R. de and Leun J. C. van der (1996) Estimates of ozone depletion and skin cancer incidence to examine the Vienna Convention achievements. Nature **384:** 256–258
3 Lima-Bessa K. M. and Menck C. F. M. (2005) Skin cancer: lights on genome lesions. Curr. Biol. **15:** R58–R61
4 Douki T. and Cadet J. (2001) Individual determination of the yield of the main UV-induced dimeric pyrimidine photoprod-

ucts in DNA suggests a high mutagenicity of CC photolesions. Biochemistry **40:** 2495–2501
5 Dulbecco R. (1949) Reactivation of ultraviolet-inactivated bacteriophage by visible light. Nature **163:** 949–950
6 Kelner A. (1949) Effect of visible light on the recovery of *Streptomyces griseus* conidia from ultraviolet-injury. Proc. Natl. Acad. Sci. USA **35:** 73–79
7 Minato S. and Werbin H. (1972) Separation of an activator of purified DNA photolyase from baker's yeast. Physiol. Chem. Phys. **4:** 467–476
8 Rupert C. S. (1960) Photoreactivation of transforming DNA by an enzyme from bakers' yeast. J. Gen. Physiol. **43:** 573–595
9 Heyes D. J., Ruban A. V., Wilks H. M. and Hunter C. N. (2002) Enzymology below 200 K: the kinetics and thermodynamics of the photochemistry catalyzed by protochlorophyllide oxidoreductase. Proc. Natl. Acad. Sci. USA **99:** 11145–11150
10 Weber S. (2004) Light-driven enzymatic catalysis of DNA repair: a review of recent biophysical studies on photolyases. Biochem. Biophys. Acta **1707:** 1–23
11 Sancar A. (2003) Structure and function of DNA photolyase and cryptochrome blue-light photoreceptors. Chem. Rev. **103:** 2203–2237
12 Cockell C. S. and Horneck G. (2001) The history of the UV radiation climate of the Earth – theoretical and space-based observations. Photochem. Photobiol. **73:** 447–451
13 Kanai S., Kikuno R., Toh H., Ryo H. and Todo T. (1997) Molecular evolution of the photolyase-blue-light photoreceptor family. J. Mol. Evol. **45:** 535–548
14 Kundu L. M., Linne U., Marahiel M. and Carell T. (2004) RNA is more UV resistant than DNA: the formation of UV-induced DNA lesions is strongly sequence and conformation dependent. Chemistry **10:** 5697–5705
15 Chinnapen D. J. F. and Sen D. (2004) A deoxyribozyme that harnesses light to repair thymine dimers in DNA. Proc. Natl. Acad. Sci. USA **101:** 65–69
16 McCready S. and Marcello L. (2003) Repair of UV damage in *Halobacterium salinarum*. Biochem. Soc. Trans. **31:** 694–698
17 Oconnor K. A., McBride M. J., West M., Yu H., Trinh L., Yuan K. et al. (1996) Photolyase of *Myxococcus xanthus*, a gram-negative eubacterium, is more similar to photolyases found in Archaea and higher eukaryotes than to photolyases of other Eubacteria. J. Biol. Chem. **271:** 6252–6259
18 Bennett C. J., Webb M., Willer D. O. and Evans D. H. (2003) Genetic and phylogenetic characterization of the type II cyclobutane pyrimidine dimer photolyases encoded by Leporipoxviruses. Virology **315:** 10–19
19 Srinivasan V., Schnitzlein W. M. and Tripathy D. N. (2001) Fowlpox virus encodes a novel DNA repair enzyme, CPD-photolyase, that restores infectivity of UV light-damaged virus. J. Virol. **75:** 1681–1688
20 Slamovits C. H. and Keeling P. J. (2004) Class II photolyase in a microsporidian intracellular parasite. J. Mol. Biol. **341:** 713–721
21 Schröder H. C., Krasko A., Gundacker D., Leys S. P., Müller I. M. and Müller W. E. G. (2003) Molecular and functional analysis of the (6-4) photolyase from the hexactinellid *Aphrocallistes vastus*. Biochem. Biophys. Acta **1651:** 41–49
22 Daiyasu H., Ishikawa T., Kuma K., Iwai S., Todo T. and Toh H. (2004) Identification of cryptochrome DASH from vertebrates. Genes Cells **9:** 479–495
23 Brudler R., Hitomi K., Daiyasu H., Toh H., Kucho K.-I., Ishiura M. et al. (2003) Identification of a new cryptochrome class: structure, function, and evolution. Mol. Cell **11:** 59–67
24 Ozgur S. and Sancar A. (2003) Purification and properties of human blue-light photoreceptor cryptochrome 2. Biochemistry **42:** 2926–2932
25 Park H. W., Kim S. T., Sancar A. and Deisenhofer J. (1995) Crystal structure of DNA photolyase from *Escherichia coli*. Science **268:** 1866–1872
26 Tamada T., Kitadokoro K., Higuchi Y., Inaka K., Yasui A., Deruiter P. E. et al. (1997) Crystal structure of DNA photolyase from *Anacystis nidulans*. Nat. Struct. Biol. **4:** 887–891
27 Komori H., Masui R., Kuramitsu S., Yokoyama S., Shibata T., Inoue Y. et al. (2001) Crystal structure of thermostable DNA photolyase: pyrimidine-dimer recognition mechanism. Proc. Natl. Acad. Sci. USA **98:** 13560–13565
28 Brautigam C. A., Smith B. S., Ma Z., Palnitkar M., Tomchick D. R., Machius M. et al. (2004) Structure of the photolyase-like domain of cryptochrome 1 from *Arabidopsis thaliana*. Proc. Natl. Acad. Sci. USA **101:** 12142–12147
29 Heelis P. F. and Sancar A. (1986) Photochemical properties of *Escherichia coli* DNA photolyase: a flash photolysis study. Biochemistry **25:** 8163–8166
30 Strassner J., Furholz A., Macheroux P., Amrhein N. and Schaller A. (1999) A homolog of old yellow enzyme in tomato – spectral properties and substrate specificity of the recombinant protein. J. Biol. Chem. **274:** 35067–35073
31 Aubert C., Vos M. H., Matthis P., Eker A. P. M. and Brettel K. (2000) Intraprotein radical transfer during photoactivation of DNA photolyase. Nature **405:** 586–590
32 Aubert C., Mathis P., Eker A. P. M. and Brettel K. (1999) Intraprotein electron transfer between tyrosine and tryptophan in DNA photolyase from *Anacystis nidulans*. Proc. Natl. Acad. Sci. USA **96:** 5423–5427
33 Weber S., Kay C. W., Mogling H., Mobius K., Hitomi K. and Todo T. (2002) Photoactivation of the flavin cofactor in *Xenopus laevis* (6-4) photolyase: observation of a transient tyrosyl radical by time-resolved electron paramagnetic resonance. Proc. Natl. Acad. Sci. USA **99:** 1319–1322
34 Giovani B., Byrdin M., Ahmad M. and Brettel K. (2003) Light-induced electron transfer in a cryptochrome blue-light photoreceptor. Nat. Struct. Biol. **10:** 489–491
35 Saxena C., Sancar A. and Zhong D. P. (2004) Femtosecond dynamics of DNA photolyase: energy transfer of antenna initiation and electron transfer of cofactor reduction. J. Phys. Chem. B **108:** 18026–18033
36 Zeugner A., Byrdin M., Bouly J.-P., Bakrim N., Giovani B., Brettel K. et al. (2005) Light-induced electron transfer in *Arabidopsis* cryptochrome-1 correlates *in vivo* function. J. Biol. Chem. **280:** 19437–19440
37 Kort R., Komori H., Adachi S., Miki K. and Eker A. P. M. (2004) DNA apophotolyase from *Anacystis nidulans:* 1.8 Å structure, 8-HDF reconstitution and X-ray-induced FAD reduction. Acta Crystallogr. D **60:** 1205–1213
38 Mees A., Klar T., Hennecke U., Eker A. P. M., Carell T. and Essen L.-O. (2004) Crystal structure of a photolyase bound to a CPD-like DNA lesion after in situ repair. Science **306:** 1789–1793
39 Kleiner O., Butenandt L., Carell T. and Batschauer A. (1999) Class II DNA photolyase from *Arabidopsis thaliana* contains FAD as a cofactor. Eur. J. Biochem. **264:** 161–167
40 Hada M., Iida Y. and Takeuchi Y. (2000) Action spectra of DNA photolyases for photorepair of cyclobutane pyrimidine dimers in sorghum and cucumber. Plant Cell Physiol. **41:** 644–648
41 Ikenaga M., Kondo S. and Fujii T. (1974) Action spectrum for enzymatic photoreactivation in maize. Photochem. Photobiol. **19:** 109–113
42 Malhotra K., Kim S. T. and Sancar A. (1994) Characterization of a medium wavelength type DNA photolyase: purification and properties of photolyase from *Bacillus firmus*. Biochemistry **33:** 8712–8718
43 Henry A. A., Jimenez R., Hanway D. and Romesberg F. E. (2004) Preliminary characterization of light harvesting in *E. coli* DNA photolyase. ChemBioChem **5:** 1088–1094
44 Kim S. T., Heelis P. F. and Sancar A. (1992) Energy transfer (deazaflavin → FADH2) and electron transfer (FADH2 → T <> T) kinetics in *Anacystis nidulans* photolyase. Biochemistry **31:** 11244–11248

45 Thoma F. (2005) Repair of UV lesions in nucleosomes – intrinsic properties and remodeling. DNA Repair **4:** 855–869
46 Ueda T., Kato A., Ogawa Y., Torizawa T., Kuramitsu S., Iwai S. et al. (2004) NMR study of repair mechanism of DNA photolyase by FAD-induced paramagnetic relaxation enhancement. J. Biol. Chem. **279:** 52574–52579
47 Torizawa T., Ueda T., Kuramitsu S., Hitomi K., Todo T., Iwai S. et al. (2004) Investigation of the cyclobutane pyrimidine dimer (CPD) photolyase DNA recognition mechanism by NMR analyses. J. Biol. Chem. **279:** 32950–32956
48 Noort J. van, Orsini F., Eker A., Wyman C., Grooth B. de and Greve J. (1999) DNA bending by photolyase in specific and non-specific complexes studied by atomic force microscopy. Nucleic Acids Res. **27:** 3875–3880
49 Husain I., Griffith J. and Sancar A. (1988) Thymine dimers bind DNA. Proc. Natl. Acad. Sci. USA **85:** 2558–2562
50 Park H., Zhang K., Ren Y., Nadji S., Sinha N., Taylor J.-S. et al. (2002) Crystal structure of a DNA decamer containing a *cis-syn* thymine dimer. Proc. Natl. Acad. Sci. USA **99:** 15965–15970
51 Harrison C. B., O'Neil L. L. and Wiest O. (2005) Computational studies of DNA photolyase. J. Phys. Chem. A **109:** 7001–7012
52 Wiest O. (1999) Structure and [2+2] cycloreversion of the cyclobutane radical cation. J. Phys. Chem. **103:** 7907–7911
53 Hahn J., Michel-Beyerle M. E. and Rösch N. (1999) Binding of pyrimidine model dimers to the photolyase enzyme: a molecular dynamics study. J. Phys. Chem. B **103:** 2001–2007
54 Gindt Y. M., Schelvis J. P. M., Thoren K. L. and Huang T. H. (2005) Substrate binding modulates the reduction potential of DNA photolyase. J. Am. Chem. Soc. **127:** 10472–10473
55 Kapentanaki S. M., Ramsey M., Gindt Y. M. and Schelvis J. P. M. (2004) Substrate electric dipole moment exerts a pH-dependent effect on electron transfer in *Escherichia coli* photolyase. J. Am. Chem. Soc. **126:** 6214–6215
56 Husain I., Sancar G. B., Holbrook S. R. and Sancar A. (1987) Mechanism of damage recognition by *Escherichia coli* DNA photolyase. J. Biol. Chem. **262:** 13188–13197
57 Kiener A., Husain I., Sancar A. and Walsh C. (1989) Purification and properties of *Methanobacterium thermoautotrophicum* DNA photolyase. J. Biol. Chem. **264:** 13880–13887
58 Vande Berg B. J. and Sancar G. B. (1998) Evidence for dinucleotide flipping by DNA photolyase. J. Biol. Chem. **273:** 20276–20284
59 McAteer K., Jing Y., Kao J., Taylor J.-S. and Kennedy M.-A. (1998) Solution-state structure of a DNA dodecamer duplex containing a *cis-syn* thymine cyclobutane dimer, the major UV photoproduct of DNA. J. Mol. Biol. **282:** 1013–1032
60 Fuxreiter M., Luo N., Jedlovszky P., Simon I. and Osman R. (2002) Role of base flipping in specific recognition of damaged DNA by repair enzymes. J. Mol. Biol. **323:** 823–834
61 Heelis P. F., Hartman R. F. and Rose S. D. (1995) Photoenzymic repair of UV-damaged DNA – a chemists perspective. Chem. Soc. Rev. **24**
62 Kao Y.-T., Saxena C., Wang L., Sancar A. and Zhong D. (2005) Direct observation of thymine dimer repair in DNA by photolyase. Proc. Natl. Acad. Sci. USA **102:** 16128–16132
63 MacFarlane A. W. and Stanley R. J. (2003) Cis-syn thymidine dimer repair by DNA photolyase in real time. Biochemistry **42:** 8558–8568
64 MacFarlane A. W. and Stanley R. J. (2001) Evidence of powerful substrate electric fields in DNA photolyase: implications for thymidine dimer repair. Biochemistry **40:** 15203–15214
65 Kavakli I. H. and Sancar A. (2004) Analysis of the role of intraprotein electron transfer in photoreactivation by DNA photolyase *in vivo*. Biochemistry **43:** 15103–15110
66 Rak J., Voityuk A. A., Michel-Beyerle M.-E. and Rösch N. (1999) Effect of proton transfer on the anionic and cationic pathways of pyrimidine photodimer cleavage, a computational study. J. Phys. Chem. A **103:** 3569–3574
67 Kim S. T. and Sancar A. (1991) Effect of base, pentose, and phosphodiester backbone structures on binding and repair of pyrimidine dimers by *Escherichia coli* DNA photolyase. Biochemistry **30:** 8623–8630
68 Schleicher E., Heßling B., Illarionova V., Bacher A., Weber S., Richter G. et al. (2005) Light-induced reactions of *Escherichia coli* DNA photolyase monitored by Fourier transform infrared spectroscopy. FEBS J. **272:** 1–12
69 Kleine T., Lockhart P. and Batschauer A. (2003) An *Arabidopsis* protein closely related to *Synechocystis* cryptochrome is targeted to organelles. Plant J. **35:** 93–103
70 Kim S. T., Malhotra K., Smith C. A., Taylor J. S. and Sancar A. (1994) Characterization of (6-4) photoproduct DNA photolyase. J. Biol. Chem. **269:** 8535–8540
71 Hitomi K., Nakamura H., Kim S. T., Mizukoshi T., Ishikawa T., Iwai S. et al. (2001) Role of two histidines in the (6-4) photolyase reaction. J. Biol. Chem. **276:** 10103–10109
72 Schul W., Jans J., Rijksen Y. M. A., Klemann K. H. M., Eker A. P. M., Wit J. N. de, et al. (2002) Enhanced repair of cyclobutane pyrimidine dimers and improved UV resistance in photolyase transgenic mice. EMBO J. **21:** 4719–4729
73 Jans J., Schul W., Sert Y. G., Rijksen Y., Rebel H., Eker A. P. M. et al. (2005) Powerful skin cancer protection by a CPD-photolyase transgene. Curr. Biol. **15:** 105–115
74 Stege H., Roza L., Vink A. A., Grewe M., Ruzicka T., Grether-Beck S. et al. (2000) Enzyme plus light therapy to repair DNA damage in ultraviolet-B-irradiated human skin. Proc. Natl. Acad. Sci. USA **97:** 1790–1795
75 Nakajima S., Lan L., Kanno S., Takao M., Yamamoto K., Eker A. P. M. et al. (2004) Light-induced DNA damage and tolerance for the survival of nucleotide excision repair-deficient human cells. J. Biol. Chem. **279:** 46674–46677
76 Zhao X., Liu J., Hsu D. S., Zhao S., Taylor J. S. and Sancar A. (1997) Reaction mechanism of (6-4) photolyase. J. Biol. Chem. **272:** 32580–32590